

On the importance of the 1-loop finite corrections to seesaw neutrino masses

D. Aristizabal Sierra^a and Carlos E. Yaguna^b

^a*IFPA, Dep. AGO, Universite de Liege,
Bat B5, Sart Tilman B-4000 Liege 1, Belgium*

^b*Institut für Theoretische Physik und Astrophysik, Universität Würzburg,
97074 Würzburg, Germany*

E-mail: daristizabal@ulg.ac.be, carlos.yaguna@physik.uni-wuerzburg.de

ABSTRACT: In the standard seesaw mechanism, finite corrections to the neutrino mass matrix arise from 1-loop self-energy diagrams mediated by a heavy neutrino. We study in detail these corrections and demonstrate that they can be very significant, exceeding in several cases the tree-level result. We consider the normal and inverted hierarchy spectra for light neutrinos and compute the finite corrections to the different elements of the neutrino mass matrix. Special attention is paid to their dependence on the parameters of the seesaw model. Among the cases in which the corrections can be large, we identify the fine-tuned models considered previously in the literature, where a strong cancellation between the different parameters is required to achieve compatibility with the experimental data. As a particular example, we also analyze how these corrections modify the tribimaximal mixing pattern and find that the deviations may be sizable, in particular for θ_{13} . Finally, we emphasize that due to their large size, the finite corrections to neutrino masses have to be taken into account if one wants to properly scan the parameter space of seesaw models.

KEYWORDS: Neutrino Physics, Beyond Standard Model

ARXIV EPRINT: [1106.3587](https://arxiv.org/abs/1106.3587)

Contents

1	Introduction	1
2	The standard seesaw model at tree level	2
3	Finite one loop corrections to the neutral fermion mass matrix	4
4	Corrections for the normal hierarchy spectrum	6
4.1	<i>R</i> real	6
4.2	<i>R</i> complex	7
5	Corrections for the inverted hierarchy spectrum	10
5.1	<i>R</i> real	10
5.2	<i>R</i> complex	11
6	A specific example: tribimaximal mixing	11
7	Discussion	13
8	Conclusions	16
A	Finite self-energy functions	16

1 Introduction

Neutrino oscillation experiments have firmly established that neutrinos have tiny but non-zero masses and that the mixing in the leptonic sector is in sharp contrast with the small mixing that characterizes the quark sector [1, 2]. From a theoretical perspective the smallness of neutrino masses can be well understood within the seesaw model [3–7], in which the fermion sector of the Standard Model is extended by adding new electroweak fermionic singlets (standard seesaw model). In this framework, light neutrino masses are generated via mixing with the singlet states and their smallness can naturally be explained if the singlets masses are very large.

The determination of the regions of parameter space consistent with low energy neutrino observables in the seesaw model typically relies on parametrizations of the neutrino Yukawa couplings [8, 9]. Once the Yukawas are properly parametrized, such regions are found by doing numerical scans in which the neutrino experimental data is used as an input. This procedure is always based on the tree-level light neutrino mass matrix and fails if in some regions of the parameter space the one-loop corrections to the tree-level mass matrix turn out to have sizable values.

The one-loop corrections to the seesaw light neutrino mass matrix were first discussed in [10] in a general setup with an arbitrary number of singlets, lepton doublets and Higgs doublets. They were later analyzed in ref. [11] in a particular realization in which, due to a particular Yukawa mass matrix, light neutrino masses vanish at tree-level and are entirely generated by the one-loop corrections. Subsequently, the renormalization of general theories with Dirac and/or Majorana neutrinos was carried out in [12] and additional studies were done in references [13–17].

Loop corrections are of two types: renormalizable and intrinsically finite. The renormalizable pieces consist of corrections to the tree level parameters already present in the seesaw Lagrangian, and are suppressed with respect to the tree level piece by extra Yukawa couplings and by the loop factor $1/16\pi^2$. The finite parts instead are corrections to the vanishing elements of the tree-level mass matrix for the neutral fermions, and are only suppressed by the loop factor. Thus, they are potentially large.

The aim of this paper is to quantify the impact that the finite one-loop corrections might have on the effective light neutrino mass matrix. We consider the most general standard seesaw model and numerically analyze the importance of these corrections for the different mass matrix elements as well as for the neutrino mass eigenvalues and mixing angles, differentiating in our discussion between the normal and the inverted light neutrino mass spectrum. We will show that the corrections can range over several orders of magnitude, depending on whether one relies or not on models where consistency with the measured neutrino masses and mixing angles requires strong cancellations in the tree-level neutrino mass matrix. Indeed, as we will discuss, once one-loop corrections are taken into account these models are barely reconcilable with data. Barring these cases, we will prove that the finite corrections are usually of order 20 – 40% but they may exceed the tree-level value for certain entries that can be strongly suppressed. In order to make reliable predictions in the seesaw, therefore, the finite one-loop corrections should be included.

The rest of the paper is organized as follows: in section 2 we define our notation and briefly describe the seesaw model at tree-level, including its standard parametrization. We discuss the finite 1-loop corrections in section 3. In sections 4 and 5 our main results are presented — the calculation of the finite corrections for the normal and inverted light neutrino mass spectrum. Then, we consider the particular case of tribimaximal mixing in section 6 and we determined how such mixing pattern is modified by the 1-loop finite corrections. A brief discussion of our results and some comments on their possible phenomenological implications is given in section 7. In section 8 we draw our conclusions and summarize our findings. For completeness, in the appendix we present the details of the calculation of the finite one-loop corrections.

2 The standard seesaw model at tree level

In the standard seesaw model, three fermionic electroweak singlets N_{R_i} are added to the Standard Model. In the basis in which the matrix of charged lepton Yukawa couplings and the singlet mass matrix are diagonal the Lagrangian accounting for the new interactions can be written as

$$- \mathcal{L} = -i\bar{N}_{R_i} \not{\partial} N_{R_i} + \tilde{\phi}^\dagger \bar{N}_{R_i} \lambda_{ij} \ell_{Lj} + \frac{1}{2} \bar{N}_{R_i} C M_{R_i} \bar{N}_R^T + \text{h.c.} \quad (2.1)$$

where $\phi^T = (\phi^+ \phi^0)$ is the Higgs electroweak doublet, ℓ_L are the leptonic SU(2) doublets, C is the charge conjugation operator and λ is a Yukawa matrix in flavor space. In the left-handed chiral basis $\mathbf{n}_L^T = (\nu_L, (\mathbf{N}_R)^C)^T$, and once electroweak symmetry breaking is taken into account, the neutral fermion mass terms can be written as

$$- \mathcal{L}_{F^0} = \frac{1}{2} \mathbf{n}_L^T C \mathcal{M} \mathbf{n}_L + \text{h.c.} \quad (2.2)$$

where \mathcal{M} , the 6×6 neutral fermion mass matrix, is given by

$$\mathcal{M} = \begin{pmatrix} \mathbf{0} & \mathbf{M}_D^T \\ \mathbf{M}_D & \hat{\mathbf{M}}_R \end{pmatrix}, \quad (2.3)$$

with $\mathbf{M}_D = v\lambda$ ($v = \sqrt{2}M_W/g \simeq 174 \text{ GeV}$). The mass spectrum is obtained by rotating the fields to the mass eigenstate basis, denoted by χ_i , via the unitary matrix \mathbf{U} :

$$\chi_L = \mathbf{U}^\dagger \mathbf{n}_L. \quad (2.4)$$

In this basis, the Lagrangian mass terms, equation (2.2), become

$$- \mathcal{L}_{F^0} = \frac{1}{2} \bar{\chi} \hat{\mathcal{M}} P_L \chi + \text{h.c.} \quad (2.5)$$

where

$$\mathbf{U}^T \mathcal{M} \mathbf{U} = \hat{\mathcal{M}} = \text{diag}(m_{\chi_1}, \dots, m_{\chi_6}) \quad (2.6)$$

and χ_i are the physical Majorana neutrino fields. Note that by decomposing the matrix \mathbf{U} as [10, 16, 17]

$$\mathbf{U} = \begin{pmatrix} \mathbf{U}_L \\ \mathbf{U}_R^* \end{pmatrix} \quad (2.7)$$

the ν_{L_i} and N_{R_i} states can be expressed as

$$\nu_{L_i} = U_{L_{ij}} P_L \chi_j, \quad N_{R_i} = U_{R_{ij}} P_R \chi_j. \quad (2.8)$$

In the seesaw limit ($\mathbf{M}_D \ll \mathbf{M}_R$), the diagonalization of the mass matrix (2.3) gives rise to a split spectrum consisting of three heavy states with masses M_{R_i} and three light states with an effective mass matrix, $\mathbf{m}_\nu^{(\text{tree})}$, given by

$$\mathbf{m}_\nu^{(\text{tree})} = -\mathbf{M}_D^T \hat{\mathbf{M}}_R^{-1} \mathbf{M}_D. \quad (2.9)$$

The light neutrino mass spectrum, mixing angles and CP violating phases — the so-called low-energy observables — are obtained from this matrix after diagonalization:

$$\mathbf{U}_\ell^T \mathbf{m}_\nu^{(\text{tree})} \mathbf{U}_\ell = \hat{\mathbf{m}}_\nu, \quad (2.10)$$

where \mathbf{U}_ℓ is the leptonic mixing matrix parametrized according to

$$\mathbf{U}_\ell = \mathbf{U}_\ell(\theta_{23}) \mathbf{U}_\ell(\theta_{13}, \delta) \mathbf{U}_\ell(\theta_{12}) \times \text{diag}(e^{-i\varphi_1}, e^{-i\varphi_2}, 1) \quad (2.11)$$

with $\delta, \varphi_{1,2}$ being respectively the Dirac and Majorana CP violating phases and $U_\ell(\theta)$ rotation matrices.

The determination of the seesaw parameters compatible with neutrino experimental data relies on parametrizations of the Yukawa couplings or, equivalently, of the Dirac neutrino mass matrix, $\mathbf{M}_D = v \lambda$. In the numerical analysis of the finite one-loop corrections, we have used the most common parametrization of the seesaw, the Casas-Ibarra parametrization [8]. In this parametrization, the most general \mathbf{M}_D compatible with eq. (2.9) is given by

$$\mathbf{M}_D = i \hat{\mathbf{M}}_R^{1/2} \mathbf{R} \hat{\mathbf{m}}_\nu^{1/2} \mathbf{U}_\ell^\dagger, \quad (2.12)$$

where \mathbf{R} is any orthogonal matrix. This matrix can be written as a rotation matrix determined by three complex angles.

The neutrino mass eigenvalues and the mixing matrix entering into this equation are strongly constrained by experimental data whereas the masses of the singlet neutrinos and the matrix \mathbf{R} are entirely free parameters of the seesaw model. In the numerical treatment of our results (sections 4 and 5) we also impose the perturbativity condition suggested recently in [18]:

$$\text{Tr} \left[\lambda^\dagger \lambda \right] \leq 3. \quad (2.13)$$

Now that we have reviewed the seesaw mechanism at tree level, let us take a look at the 1-loop corrections to neutrino masses.

3 Finite one loop corrections to the neutral fermion mass matrix

In the standard seesaw mechanism, the one-loop corrections to the $\nu - N$ mass matrix are determined by the neutrino interactions with the Z boson, the neutral Goldstone bosons (G^0), and the Higgs boson (h^0) — see appendix A. All together, in addition to the correction involving the standard model leptonic charged current, they define the one-loop two point function $-i\Sigma(p)$ [17].

Once the one-loop corrections are taken into account the neutral fermion mass matrix is given by

$$\mathcal{M} = \mathcal{M}^{(\text{tree})} + \mathcal{M}^{(1\text{-loop})}, \quad (3.1)$$

where the 1-loop contribution can be decomposed as

$$\mathcal{M}^{(1\text{-loop})} = \begin{pmatrix} \delta\mathbf{M}_L & \delta\mathbf{M}_D^T \\ \delta\mathbf{M}_D & \delta\mathbf{M}_R \end{pmatrix}. \quad (3.2)$$

Notice that the $\mathbf{0}_{3 \times 3}$ matrix appearing at tree-level is replaced by the contribution $\delta\mathbf{M}_L$, which among all the sub-matrices in $\mathcal{M}^{(1\text{-loop})}$ is the dominant one [17].

Neglecting the subdominant pieces in $\mathcal{M}^{(1\text{-loop})}$ and after block diagonalization of the neutral fermion mass matrix, the effective light neutrino mass matrix, up to one-loop order, can be written as

$$\mathbf{m}_\nu = \mathbf{m}_\nu^{(\text{tree})} + \mathbf{m}_\nu^{(1\text{-loop})} = -\mathbf{M}_D^T \hat{\mathbf{M}}_R^{-1} \mathbf{M}_D + \delta\mathbf{M}_L. \quad (3.3)$$

The sub-matrix $\delta\mathbf{M}_{\mathbf{L}}$ and all the other sub-matrices entering in $\mathcal{M}^{(1\text{-loop})}$ are entirely determined by the self-energy functions $\Sigma_{\mathbf{L}}^{\mathbf{S}}(p^2)$ (see appendix A) via the diagonalization relation (2.6):

$$\mathcal{M}^{(1\text{-loop})} = \mathbf{U}^* \Sigma_{\mathbf{L}}^{\mathbf{S}}(p^2) \mathbf{U}^\dagger. \quad (3.4)$$

Accordingly, the finite contribution is given by

$$\delta\mathbf{M}_{\mathbf{L}} = \mathbf{U}_{\mathbf{L}}^* \Sigma_{\mathbf{L}}^{\mathbf{S}}(p^2) \mathbf{U}_{\mathbf{L}}^\dagger = \mathbf{U}_{\mathbf{L}}^* \Sigma_{\mathbf{L}}^{\mathbf{S}}(0) \mathbf{U}_{\mathbf{L}}^\dagger, \quad (3.5)$$

where we have used the fact that $\Sigma_{\mathbf{L}}^{\mathbf{S}}$ can be evaluated at zero external momentum [17]. The self-energy functions $\Sigma_{\mathbf{L}}^{\mathbf{S}}(0)$ are determined by three Feynman self-energy diagrams involving the Z , the neutral Goldstone boson G^0 and the Higgs boson h^0 . Each diagram contains a divergent piece but when summing up the three contributions the result turns out to be finite, as it has to be since there are no counterterms that would allow to absorb a possible divergence (see appendix A for more details). The final expression for the finite one-loop correction is given by [17]

$$\delta\mathbf{M}_{\mathbf{L}} = \mathbf{M}_{\mathbf{D}}^T \hat{\mathbf{M}}_{\mathbf{R}}^{-1} \left\{ \frac{g^2}{64\pi^2 M_W^2} \left[m_h^2 \ln \left(\frac{\hat{M}_{\mathbf{R}}^2}{m_h^2} \right) + 3M_Z^2 \ln \left(\frac{\hat{M}_{\mathbf{R}}^2}{M_Z^2} \right) \right] \right\} \mathbf{M}_{\mathbf{D}}. \quad (3.6)$$

Notice that this correction is not suppressed, with respect to tree-level result, by additional factors of M_D/M_R . Thus, it is expected to be smaller than the tree-level mass term solely by a factor of order $(16\pi^2)^{-1} \ln(M_R/M_Z)$.

In spite of the similar structure of the 1-loop correction and the tree-level result, they are not proportional to each other unless the heavy neutrinos are degenerate — $\mathbf{M}_{\mathbf{R}} \propto \mathbf{I}$. Hence, one could in principle have that $\mathbf{m}_\nu^{(\text{tree})} = 0$ and that neutrino masses arise entirely from 1-loop effects, as proposed in [11]. Such models, however, are rather contrived and will not be discussed in the following. We are interested, instead, in the generic modifications to the neutrino mass matrix induced by the 1-loop corrections.

To evaluate these corrections, we first find sets of $\mathbf{M}_{\mathbf{D}}$ and $\hat{\mathbf{M}}_{\mathbf{R}}$ compatible with the experimental data at tree-level — using equation (2.12) — and then use them to evaluate $\delta\mathbf{M}_{\mathbf{L}}$.¹ Specifically, we generate the diagonal matrix of light neutrino masses (according to the desired spectra: normal or inverted) and the mixing matrix \mathbf{U}_ℓ such that they are compatible with neutrino data. For simplicity, the phases in \mathbf{U}_ℓ were assumed to vanish. Then, we randomly generate the three masses of the heavy states (in the range 1 TeV to 10^{12} GeV) and the elements of the orthogonal matrix \mathbf{R} . From equation (2.12), we can then obtain $\mathbf{M}_{\mathbf{D}}$, which together with the generated $\mathbf{M}_{\mathbf{R}}$ allows us to evaluate $\delta\mathbf{M}_{\mathbf{L}}$.² The size of the corrections is then determined by the ratio between the contributions up to 1-loop order and the tree-level result for the different elements of the neutrino mass matrix, $(\mathbf{m}_\nu^{(\text{tree})} + \mathbf{m}_\nu^{(1\text{-loop})})/\mathbf{m}_\nu^{(\text{tree})}$.

In the next two sections our main results are presented: we compute the corrections to the neutrino mass matrix in the seesaw model for the two different kinds of light neutrino spectra, with normal and inverted hierarchy.

¹Alternatively, one could choose the seesaw parameters so that at 1-loop they are compatible with the experimental data. Both procedures give rise to the same effects.

²In our analysis we fix $m_{h^0} = 150$ GeV.

4 Corrections for the normal hierarchy spectrum

If the spectrum of light neutrinos has a normal hierarchy ($m_{\nu_3} = \sqrt{\Delta m_{\text{atm}}^2}$, $m_{\nu_2} = \sqrt{\Delta m_{\text{sol}}^2}$, $m_{\nu_1} \ll m_{\nu_2}, m_{\nu_3}$), the elements of the neutrino mass matrix take values within the following ranges:

$$\mathbf{m}_\nu^{\text{exp}} = \begin{pmatrix} (2.5, 5.5) \times 10^{-12} & (2.3, 9.8) \times 10^{-12} & (-3.3, 4.9) \times 10^{-12} \\ - & (2.0, 3.4) \times 10^{-11} & (1.9, 2.3) \times 10^{-11} \\ - & - & (2.1, 3.4) \times 10^{-11} \end{pmatrix} \text{ GeV} \quad (4.1)$$

as the oscillation parameters vary within their $2\text{-}\sigma$ experimentally allowed intervals [1, 2]. Since the matrix is symmetric, we only show the six independent matrix elements. Notice, in particular, that the element (1,3) is the only one that can vanish in this case. It can be easily checked that this can happen if θ_{13} is between 4° and 6° . All other elements vary within a relatively small range — not so small for (1,2) — between 10^{-11} and 10^{-12} GeV. Since the corrections to the neutrino mass matrix are not proportional to the matrix element itself, the correction to the element (1,3) could easily exceed its tree-level value.

With the aim of facilitating the study of these corrections and the understanding of their origin, we will divide our analysis in two parts depending on what is assumed for the orthogonal matrix \mathbf{R} . First it is taken to be real and then the most general case is considered, a complex matrix. The number of free parameters will therefore increase as we move from the first case to the second.

4.1 \mathbf{R} real

If \mathbf{R} is real, the parameters needed to evaluate the 1-loop correction to the neutrino mass matrix are the oscillation parameters, the three masses of the right handed neutrinos (M_i), and the three angles that parametrize \mathbf{R} . To obtain the numerical results below, we vary the neutrino mixing angles and mass squared differences within their 2σ ranges, and we randomly choose M_i between 1 TeV and 10^{12} GeV and the angles in \mathbf{R} between 0 and 2π .

The resulting corrections to the matrix elements are shown in figure 1 as a function of the mass of the lightest heavy neutrino, M_1 . We see that they are similar for the elements (1,1), (2,2), (2,3), and (3,3), increasing with M_1 and reaching values up to order 30%. Those for the element (1,2) are slightly different, reaching values as large as 40% or 50% as well as -20% .

The corrections to the element (1,3), on the other hand, can be quite large for a significant fraction of models. As anticipated, this result is due to the fact that the element (1,3) can be very small so it may receive a huge fractional correction. It must be noticed in that case, however, that a large value of $(\mathbf{m}_\nu^{(\text{tree})} + \mathbf{m}_\nu^{(1\text{-loop})})/\mathbf{m}_\nu^{(\text{tree})}$ does not necessarily imply a significant deviation in the expected value of the neutrino observables — the mass eigenvalues and the mixing angles. For that reason it is important to study the effect of the corrections on both the matrix elements and the predicted observables. We will do so in the next section, where we consider the most general case: \mathbf{R} complex.

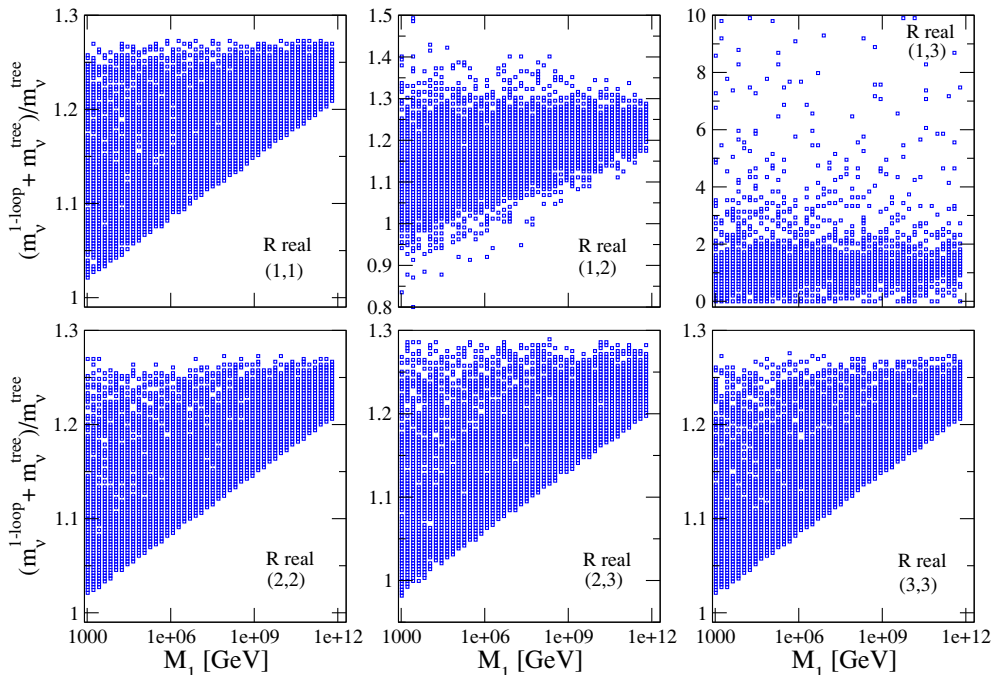


Figure 1. The ratio between the 1-loop and the tree-level result for the different elements of the neutrino mass matrix as a function of M_1 . It has been assumed that \mathbf{R} is real and that light neutrinos have a NH spectrum.

Notice then that even in the case \mathbf{R} real, where no large parameters are introduced, the corrections to neutrino masses can be quite important. If $M_1 \gtrsim 10^9$ GeV they are expected to be larger than about 15% and they could easily reach 25% or 30%.

4.2 \mathbf{R} complex

This case is not only the most general one, but it is also well motivated by leptogenesis. In fact, in the case of unflavored leptogenesis, the phases in \mathbf{R} are the ones responsible for the CP-asymmetry in the decays of the heavy neutrinos and ultimately for the generation of the baryon asymmetry.

In this case, the three angles parametrizing \mathbf{R} are complex numbers, with a certain magnitude and a given phase. In our analysis, we allow these complex angles to have an arbitrary phase and we restrict their magnitude to be smaller than 3.³ Since $\cosh 3 \sim \sinh 3 \sim 10$, \mathbf{R} can have elements at most of order 10^3 . When the elements of \mathbf{R} are significantly larger than 1, $|R_{ij}| \gg 1$, one obtains the so-called fine-tuned models. In them, strong cancellations between the different terms in equation (2.9) are required to obtain compatibility with the experimental data. Since the corrections to the neutrino mass matrix depend on \mathbf{R} , the loop suppression in (3.6) can be easily overcome by the large elements in \mathbf{R} , yielding a correction that is significantly larger than the tree level result.

³One can relax this assumption to obtain even larger effects.

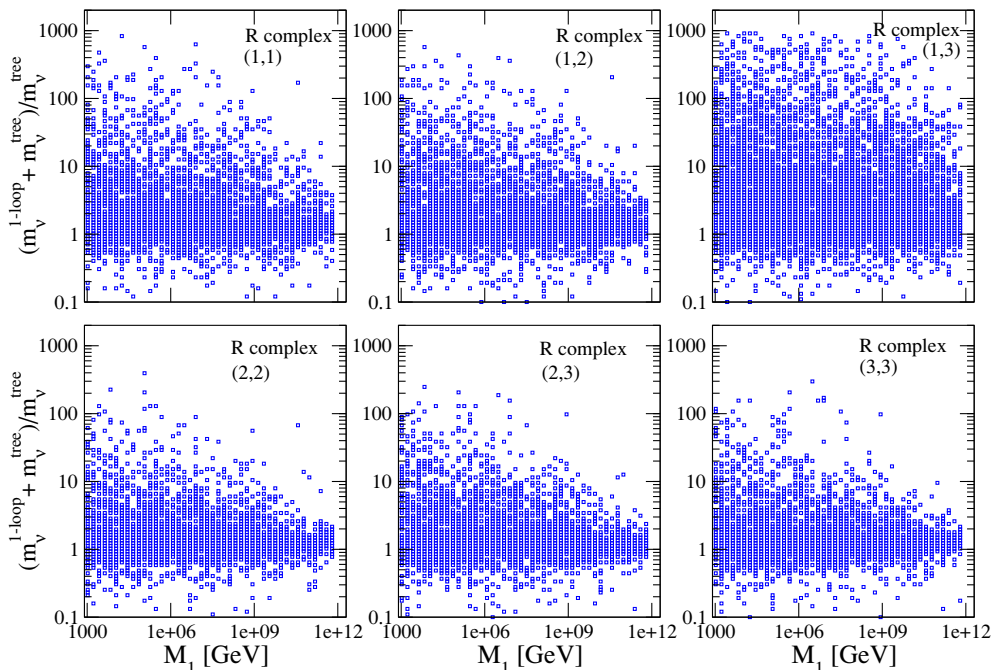


Figure 2. The ratio between the 1-loop and the tree-level result for the different elements of the neutrino mass matrix as a function of M_1 . It has been assumed that \mathbf{R} is complex and that light neutrinos have a NH spectrum.

Figure 2 shows the corrections to the different matrix elements for \mathbf{R} complex. We see that, in fact, the 1-loop contribution can exceed, for all the matrix elements, the tree-level result by several orders of magnitude. In that case, there is no doubt that the corrections will have a huge impact on the predicted neutrino mass eigenvalues and mixing angles.

It is indeed the large elements present in \mathbf{R} that make possible a 1-loop correction much larger than the tree-level result. We illustrate this fact in figure 3, which shows the size of the corrections as a function of the largest element of the \mathbf{R} matrix, $|R_{ij}|_{\max}$. Notice that when this element is of order 1 the corrections are usually small (those to the element (1,3) being the exception) but they increase with it reaching two orders of magnitude or more for $|R_{ij}|_{\max}$ around 100. With such huge corrections, the agreement between the tree-level seesaw formula and the neutrino data assumed in the parametrization becomes meaningless. In fact, as illustrated in figures 4 and 5, the oscillation parameters may deviate significantly from their observed values once the 1-loop corrections are taken into account.

Figure 4 displays the 1-loop mixing angles, those obtained from the diagonalization of the neutrino mass matrix at 1-loop, as a function of $|R_{ij}|_{\max}$. The region consistent with the experimental data at 2σ is the area between the two dashed lines. Notice that all the angles, which were chosen to be consistent with the data at tree level, can at 1-loop become much larger than allowed by present observations.

Similarly, we see in figure 5 that the neutrino mass squared differences at 1-loop can vary over several orders of magnitude. A fact that is in clear contradiction with current experiments.

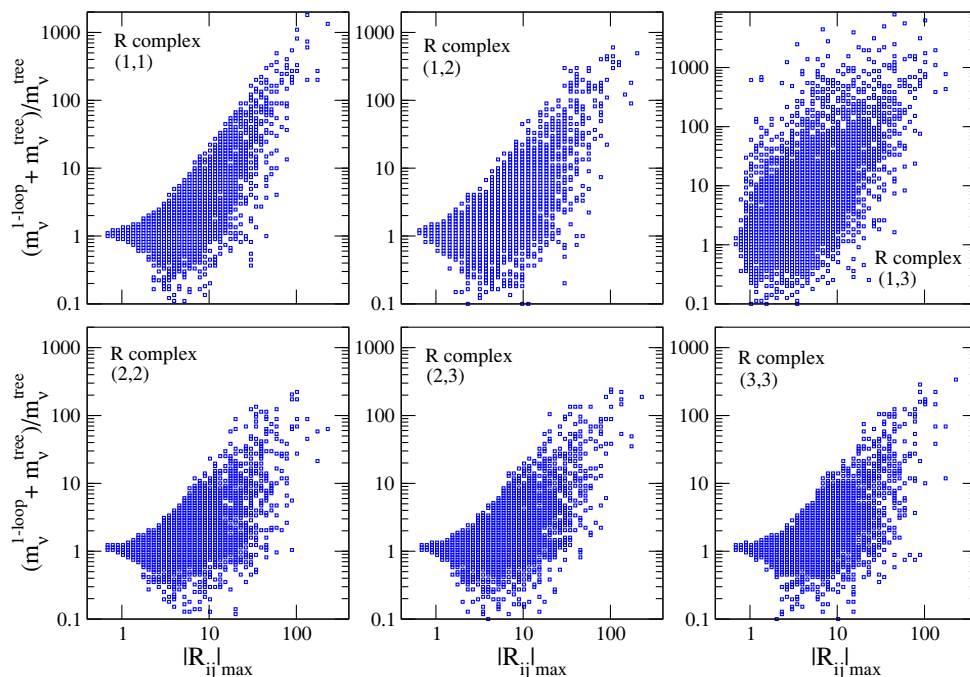


Figure 3. The ratio between the 1-loop and the tree-level result for the different elements of the neutrino mass matrix as a function of the largest element of the \mathbf{R} matrix. It has been assumed that \mathbf{R} is complex and that light neutrinos have a NH spectrum.

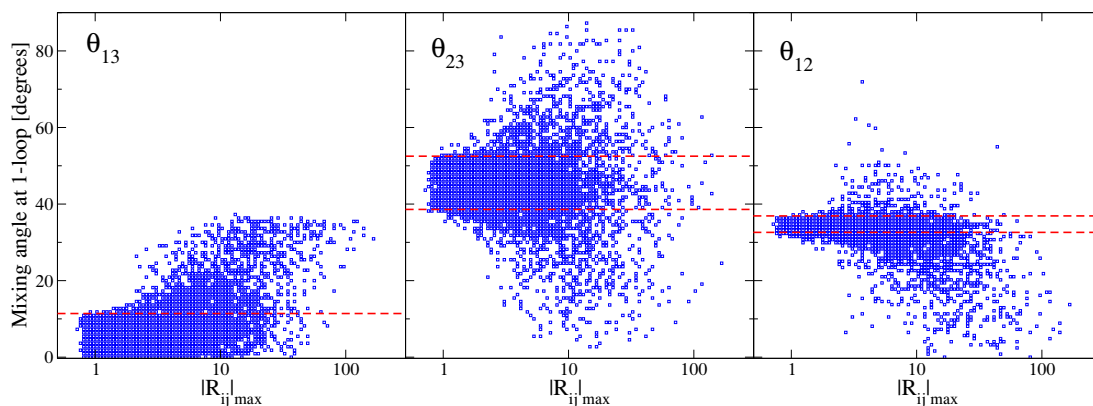


Figure 4. The neutrino mixing angles at 1-loop as a function of the largest element of the \mathbf{R} matrix. It has been assumed that \mathbf{R} is complex and that light neutrinos have a NH spectrum. The region between the two dashed (red) lines is consistent with current experimental data at 2σ .

As we have seen, for the neutrino spectrum with normal hierarchy the corrections to the neutrino mass matrix can be quite important. The matrix element (1, 3), in particular, can receive very large fractional corrections independently of \mathbf{R} if $m_{\nu 13}$ is suppressed. In addition, all matrix elements as well as the neutrino mass eigenvalues and mixing angles are expected to receive significant corrections when the elements of the \mathbf{R} matrix are larger than one. In such case, the inclusion of the 1-loop corrections is mandatory.

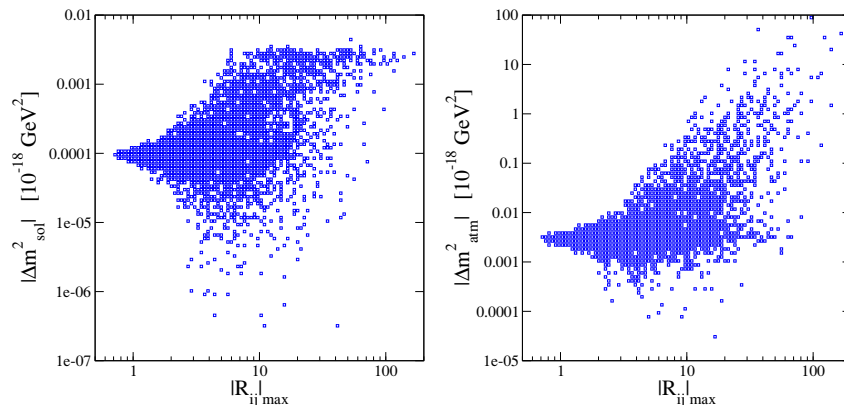


Figure 5. The neutrino mass squared differences at 1-loop as a function of the largest element of the \mathbf{R} matrix. It has been assumed that \mathbf{R} is complex and that light neutrinos have a NH spectrum.

Next, we analyze the importance of these corrections for the neutrino spectrum with inverted hierarchy.

5 Corrections for the inverted hierarchy spectrum

If the spectrum of light neutrinos has an inverted hierarchy (IH), $m_{\nu_2} = \sqrt{|\Delta m_{\text{atm}}^2|}$, $m_{\nu_1} = \sqrt{|\Delta m_{\text{atm}}^2| - \Delta m_{\text{sol}}^2}$, $m_{\nu_3} \ll m_{\nu_2}, m_{\nu_1}$, the elements of the neutrino mass matrix take values within the following ranges:

$$\mathbf{m}_\nu^{\text{exp}} = \begin{pmatrix} (4.5, 5.1) \times 10^{-11} & (-8.5, 1.7) \times 10^{-12} & (-8.5, 1.3) \times 10^{-12} \\ - & (1.7, 3.3) \times 10^{-11} & (-2.5, -2.0) \times 10^{-11} \\ - & - & (1.8, 3.4) \times 10^{-11} \end{pmatrix} \text{ GeV} \quad (5.1)$$

as the oscillation parameters vary within their $2\text{-}\sigma$ experimentally allowed intervals [1, 2]. Notice that in this case the elements (1, 2) and (1, 3) are both allowed to vanish, an event that can happen if θ_{13} is smaller than about 2° . We expect, therefore, large fractional corrections to the entries (1, 2) and (1, 3) of the neutrino mass matrix independently of \mathbf{R} . As before, we will divide the analysis of the 1-loop corrections into two parts: \mathbf{R} real and \mathbf{R} complex.

5.1 \mathbf{R} real

The finite corrections for \mathbf{R} real are shown, as a function of M_1 , in figure 6. The range of variation is approximately the same for the elements (2, 2), (2, 3), (3, 3), and (1, 1), reaching maximum values of order 30% independently of M_1 . The minimum value of the correction, on the other hand, is seen to increase with M_1 . The entries (1, 2) and (1, 3) may feature large fractional corrections, a consequence of the vanishing matrix elements at tree-level. Comparing these results with those obtained in the previous section, it is evident that the type of light neutrino spectrum does not have a decisive impact on the generic size or behavior of the finite corrections.

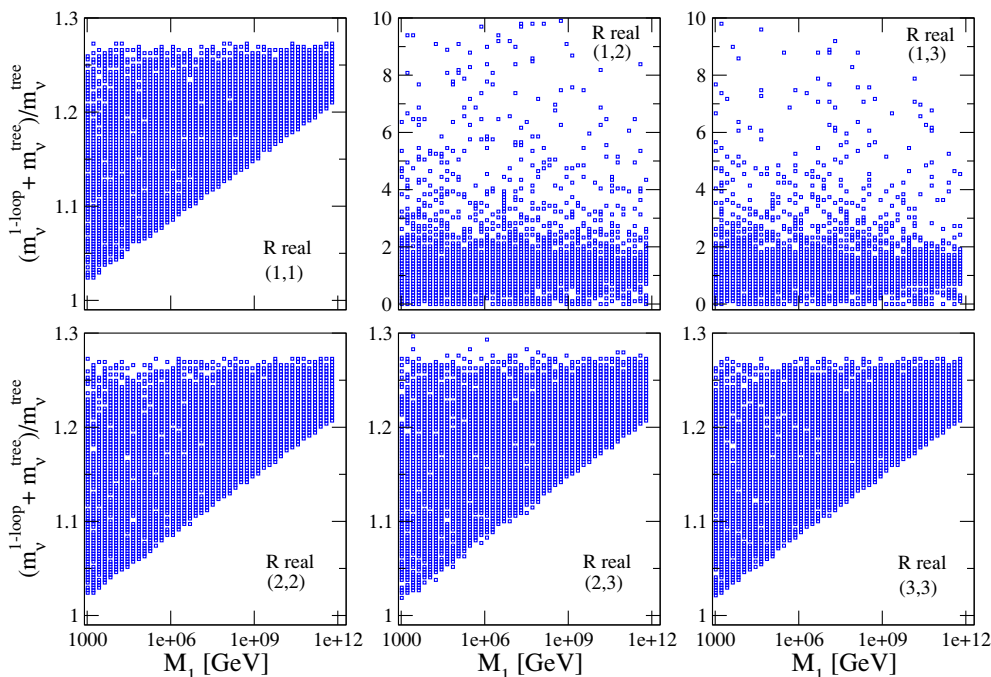


Figure 6. The ratio between the 1-loop and the tree-level result for the different elements of the neutrino mass matrix as a function of M_1 . It has been assumed that \mathbf{R} is real and that light neutrinos have a IH spectrum.

5.2 R complex

In the most general case of a complex \mathbf{R} matrix, the corrections tend to be quite large for all entries, as illustrated by figure 7. They can easily reach 2 or 3 orders of magnitude above the tree-level value, being typically larger for the (1,2) and (1,3) matrix elements. They may also give rise to cancellations between the tree-level and the 1-loop contribution, such that the full result at 1-loop could only be a small fraction of the tree-level result — see e.g. the points around 0.1 in the figure.

These large fractional corrections to the elements of the neutrino mass matrix translate into important deviations in the neutrino mass eigenvalues and the neutrino mixing angles, just as for the spectrum with normal hierarchy — see previous section.

For a light neutrino spectrum with inverted hierarchy, therefore, the corrections are even more important than for the normal hierarchy spectrum, as there are two different matrix elements that can receive large fractional corrections independently of \mathbf{R} . If \mathbf{R} contains large numbers then the corrections to all matrix elements are usually significant for both the normal and the inverted hierarchy spectrum.

6 A specific example: tribimaximal mixing

We would like now to apply the ideas discussed in the previous sections to a particular and well-motivated scenario: seesaw models with tribimaximal mixing (see e.g. [19]). In

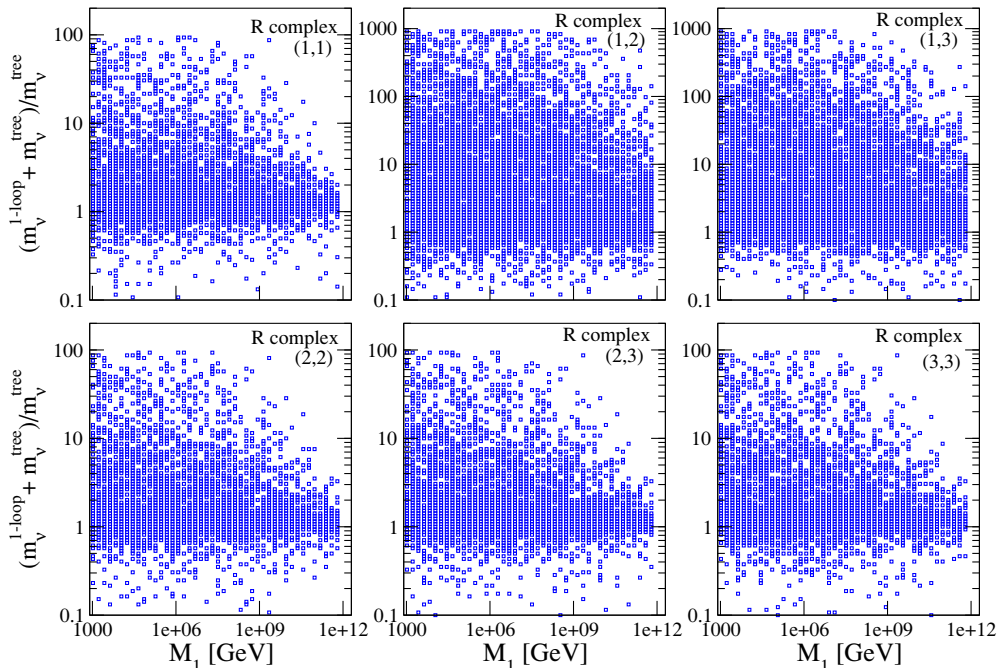


Figure 7. The ratio between the 1-loop and the tree-level result for the different elements of the neutrino mass matrix as a function of M_1 . It has been assumed that \mathbf{R} is complex and that light neutrinos have a IH spectrum.

scenarios with tribimaximal mixing, the neutrino mixing matrix is given at tree level by

$$U_\ell = \begin{pmatrix} \sqrt{2/3} & 1/\sqrt{3} & 0 \\ -1/\sqrt{6} & 1/\sqrt{3} & -1/\sqrt{2} \\ -1/\sqrt{6} & 1/\sqrt{3} & 1/\sqrt{2} \end{pmatrix}. \tag{6.1}$$

As a result, the mixing angles take the values $\theta_{12} = 35.3^\circ$, $\theta_{23} = 45^\circ$, $\theta_{13} = 0$ at tree level. One may therefore wonder how they would change once the finite one-loop corrections to the seesaw neutrino mass matrix that we have studied are taken into account.⁴ For simplicity, we will limit ourselves in this section to the normal hierarchy spectrum and to the case \mathbf{R} real. Larger corrections are expected if \mathbf{R} is complex.

Figure 8 shows the 1-loop value of θ_{23} as a function of the lightest heavy neutrino mass. We see that it can deviate from its tree-level value by up to 2.5 degrees and that the maximum deviation decreases with M_1 . In fact, for $M_1 \gtrsim 10^{12}$ GeV the correction is smaller than half a degree. This dependence with M_1 is very different to that observed for the matrix elements but it is consistent with it. Since the mixing angles are determined by ratios between different matrix elements, in order to have a sizable variation in the mixing angles, the structure of the neutrino mass matrix should vary significantly at 1-loop, implying that the correction should not be proportional to the identity. Hence, in

⁴Additional corrections from other sources may also be important but are not considered here.

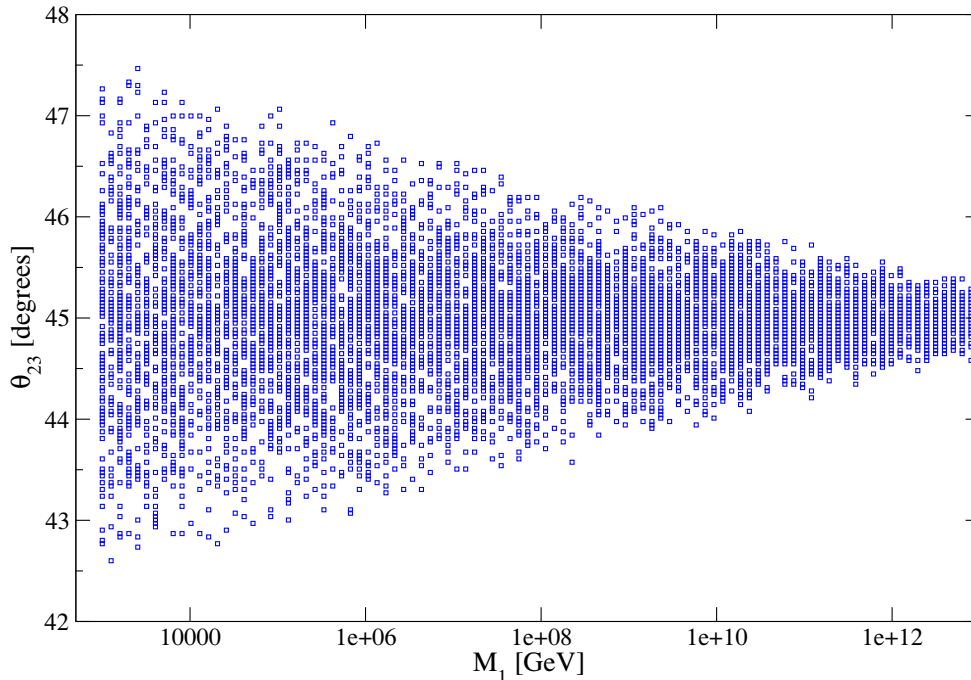


Figure 8. The mixing angle θ_{23} at 1-loop as a function of the lightest heavy neutrino. At tree level θ_{23} was assumed to be 45° , in agreement with the tribimaximal mixing pattern.

models where there is a large hierarchy between the masses of the heavy neutrinos, the corrections to the mixing angles are larger. That is exactly what is observed in figure 8.

The 1-loop corrected value of θ_{12} is shown in figure 9 as a function of M_1 . The variation in this case is smaller and it also decreases with M_1 . More interesting for the phenomenology of neutrinos and for future experiments is the correction to θ_{13} , which is exactly zero at tree level. Figure 10 shows that the 1-loop corrected value of θ_{13} can reach almost 2 degrees, corresponding to $\sin^2 \theta_{13} \sim 10^{-3}$, for M_1 around 1 TeV. As expected, the maximum correction decreases with M_1 , amounting to about 1 degree ($\sin^2 \theta_{13} \sim 3 \times 10^{-4}$) for $M_1 \sim 10^8$ GeV. Given that a neutrino factory could be sensitive to $\sin^2 \theta_{13} \sim 10^{-5}$ [20], these corrections are certainly within the reach of future experiments.

7 Discussion

The huge corrections we have found for fine-tuned models are not surprising. It is well-known in the literature that radiative corrections to fine-tuned models should spoil the tuning imposed at tree-level between the different parameters (see e.g. [21]) and that it is unnatural to expect otherwise. We have explicitly shown that that is the case. The 1-loop corrections to the neutrino mass matrix in fine-tuned seesaw models are so large that the compatibility between the tree-level seesaw formula and the experimental data becomes irrelevant. The inclusion of the 1-loop corrections is in such case necessary.

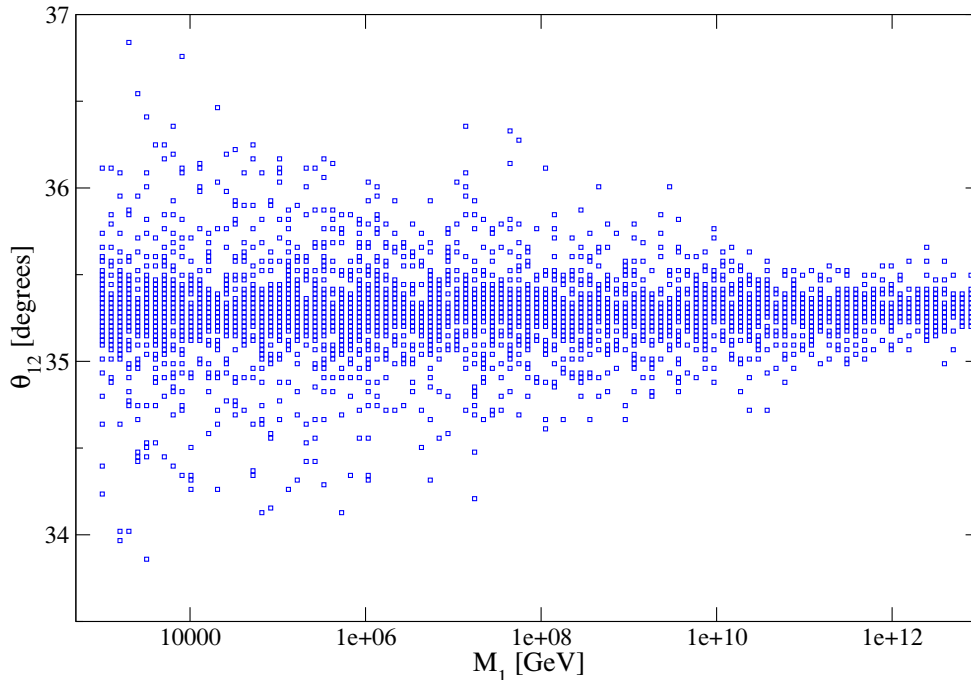


Figure 9. The mixing angle θ_{12} at 1-loop as a function of the lightest heavy neutrino. At tree level θ_{12} was assumed to be 35.3° , in agreement with the tribimaximal mixing pattern.

As a way of avoiding such large corrections, one may think of including the 1-loop correction into the seesaw parametrization from the very beginning. That is, one would like to look for the most general solution to equation (3.3) rather than to equation (2.9). Doing so, however, would not completely solve the problem. We would, instead, be constructing fine-tuned models at the 1-loop level, which are expected to receive large corrections at 2-loops. Fine-tuned models, it seems, are better avoided.

One possibility to do so is simply to restrict from the very beginning the magnitude of the complex angles that parametrize \mathbf{R} . If they are such that $|R_{ij}|_{\max} \lesssim 1$ then no fine-tuning occurs and the corrections are usually under control. This additional restriction, however, has not been taken into account in previous analysis. And it was recently suggested in [18] that a fair scan of the seesaw parameter space is one in which no restriction beyond the perturbativity of the neutrino Yukawa couplings, which we have implemented, is imposed. Our results clearly demonstrate, on the contrary, that perturbativity is not enough to guarantee the stability of the neutrino mass matrix under radiative corrections and that wrong results can easily be reached if the 1-loop corrections are not taken into account. In fact, as we have seen, a significant fraction of models which are compatible with the data at tree level are no longer so once the 1-loop corrections are considered. Thus, when one is randomly scanning the parameter space of the seesaw model, it is necessary to include the finite corrections to neutrino masses.

Another possible way out is the use of a different parametrization. An alternative to the \mathbf{R} parametrization that has been used in previous works is the V_L parametrization. In

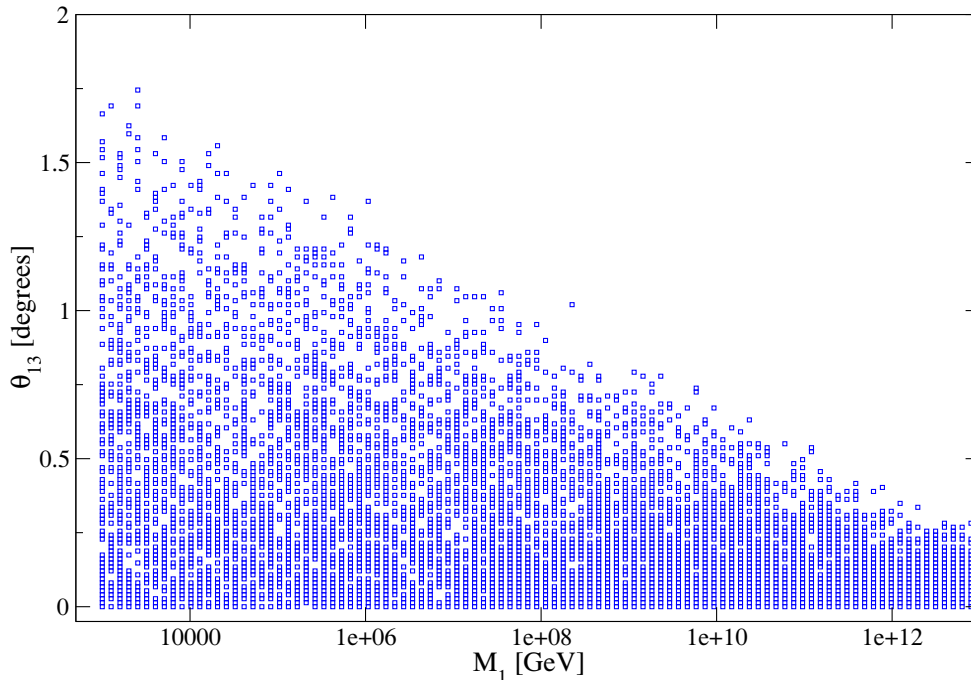


Figure 10. The mixing angle θ_{13} at 1-loop as a function of the lightest heavy neutrino. At tree level θ_{13} was assumed to vanish, in agreement with the tribimaximal mixing pattern.

it, \mathbf{M}_D is written as

$$\mathbf{M}_D = \mathbf{V}_R^\dagger \hat{\mathbf{M}}_D \mathbf{V}_L, \quad (7.1)$$

where $\hat{\mathbf{M}}_D$ is a diagonal matrix defined by the eigenvalues of \mathbf{M}_D (real and positive) and $\mathbf{V}_{L,R}$ are unitary matrices determined by three rotation angles and three complex phases. In this parametrization, $\hat{\mathbf{M}}_D$, \mathbf{V}_L and the neutrino data are used as inputs. Using equation (7.1) and the effective light neutrino mass matrix the following relation is obtained

$$\hat{\mathbf{M}}_D^{-1} \mathbf{V}_L^* \mathbf{m}_\nu^{(\text{tree})} \mathbf{V}_L^\dagger \hat{\mathbf{M}}_D^{-1} = \mathbf{V}_R^* \hat{\mathbf{M}}_R^{-1} \mathbf{V}_R^\dagger, \quad (7.2)$$

which allows us to determine \mathbf{V}_R and $\hat{\mathbf{M}}_R$ for a given set of input parameters. We have computed the corrections to the neutrino mass matrix also in this parametrization, and have observed that the results for $\mathbf{R} = \mathbf{I}$ and \mathbf{R} real are easily reproduced for $\mathbf{V}_L = \mathbf{I}$ and \mathbf{V}_L real. In particular, the large corrections for certain matrix elements are obtained there too. An important difference occurs, however, for \mathbf{R} complex. Due to the different way in which the \mathbf{V}_L parametrization samples the parameter space of the seesaw model, it is way more difficult to find fine-tuned models, with the consequence that models with very large corrections are rather scarce in the \mathbf{V}_L parametrization.

In a future publication, we will discuss additional implications of these corrections, including their evaluation in supersymmetric scenarios as well as their possible effects in leptogenesis and lepton flavor violating processes.

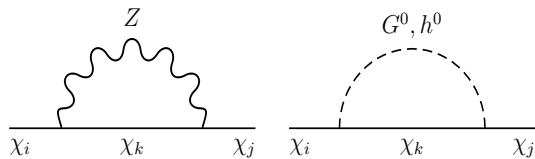


Figure 11. Self-energy diagrams accounting for $\delta\mathbf{M}_L$

8 Conclusions

The seesaw model is one of the most appealing extensions of the Standard Model that can explain neutrino masses. In this model, the mass matrix of light neutrinos receives finite corrections from 1-loop diagrams mediated by the heavy neutrinos. We considered the two different kinds of light neutrino spectra, hierarchical and inverted, and computed the corrections to the entries of the neutrino mass matrix as a function of the seesaw parameters. We found these corrections to be quite important, exceeding in several cases of interest the tree level result by orders of magnitude. Two different reasons were identified as leading to a large correction: an unusually suppressed tree-level result and an \mathbf{R} matrix with elements much larger than 1. Examples of the first case are the corrections to the matrix element (1, 3) for NH neutrinos and to (1, 2) and (1, 3) for IH neutrinos. The second case can occur for \mathbf{R} complex and includes the so-called fine-tuned models considered in the literature. Since these corrections can be large, models that at tree-level are compatible with the experimental neutrino data will not necessarily be so at the 1-loop level, modifying in a significant way the viable regions in the parameter space of the seesaw model. As a particular example, we studied the corrections to the mixing angles in seesaw scenarios with tribimaximal mixing and show them to lead to observable effects in future experiments. We stressed, therefore, that because of their size and importance, these corrections must necessarily be taken into account in the study and analysis of seesaw models.

Acknowledgments

We would like to thank Maria Jose Herrero, Enrico Nardi, Alejandro Ibarra and Walter Winter for useful discussions and suggestions. DAS is supported by a belgian FNRS postdoctoral fellowship. CEY is supported by DFG grant no. WI 2639/2-1.

A Finite self-energy functions

In this appendix we present the calculation of the finite 1-loop corrections $\delta\mathbf{M}_L$ discussed in section 3, we will closely follow ref. [17]. The self-energy function $\Sigma_L^S(0)$, that determines these corrections, can be written as

$$-i\Sigma_L^S(0) = -i \left[\Sigma_L^{S(Z)}(0) + \Sigma_L^{S(G^0)}(0) + \Sigma_L^{S(h^0)}(0) \right], \tag{A.1}$$

where the $\Sigma_L^{S(Z,G^0,h^0)}(0)$ functions arise from the self-energy Feynman diagrams (evaluated at zero external momentum) involving the Z , the neutral Goldstone boson G^0 and the Higgs

h^0 shown in figure 11. The calculation of these functions is determined by the coupling of the Z with the Majorana eigenstates χ :

$$\mathcal{L}_Z = \frac{g}{4c_w} Z_\mu \bar{\chi} \gamma^\mu \left[P_L (\mathbf{U}_L^\dagger \mathbf{U}_L) - P_R (\mathbf{U}_L^T \mathbf{U}_L^*) \right] \chi, \quad (\text{A.2})$$

($c_w = \cos \theta_w$ with θ_w the weak mixing angle), the couplings with the Higgs boson, derived from the Lagrangian (2.1),

$$- \mathcal{L}_{h^0} = \frac{1}{2\sqrt{2}} h^0 \bar{\chi} \left[\mathbf{O}_L^S P_L + \mathbf{O}_R^S P_R \right] \chi, \quad (\text{A.3})$$

where the couplings $\mathbf{O}_{L,R}^S$ are given by

$$\mathbf{O}_L^S = \mathbf{U}_R^\dagger \lambda \mathbf{U}_L + \mathbf{U}_L^T \lambda^T \mathbf{U}_R^* \quad (\text{A.4})$$

$$\mathbf{O}_R^S = \mathbf{U}_L^\dagger \lambda^\dagger \mathbf{U}_R + \mathbf{U}_R^T \lambda^* \mathbf{U}_L^*, \quad (\text{A.5})$$

and finally the couplings with G^0 that can be obtained from the Lagrangian (A.3) by replacing $\mathbf{O}_{L,R}^S \rightarrow -i\mathbf{O}_{L,R}^S$. From these Lagrangians and the diagonalization relation (3.4) it can be seen that $\Sigma_L^{S(Z)}(0)$ contributes only to $\delta\mathbf{M}_L$ whereas $\Sigma_L^{S(G^0, h^0)}(0)$ contribute to all the block matrices of the 6×6 neutral fermion mass matrix. The contributions of these self-energies to $\delta\mathbf{M}_L$ can be identified by means of the relation (3.5).

Using dimensional regularization ($d = 4 - \epsilon$) and working in the R_ξ gauge the Z self-energy function is found to be

$$\Sigma_L^{S(Z)}(0) = \mathbf{U}_L^T \left[\delta\mathbf{M}_L^{(Z)}(1) + \delta\mathbf{M}_L^{(Z)}(2, 1) + \delta\mathbf{M}_L^{(Z)}(2, 2) \right] \mathbf{U}_L, \quad (\text{A.6})$$

where the different matrices can be expressed in terms of the Passarino-Veltman function $B_0(0, m_0^2, m_1^2)$ [22], namely

$$\delta\mathbf{M}_L^{(Z)}(1) = -\frac{g^2}{64\pi^2 c_w^2} (4 - \epsilon) \mathbf{U}_L^* \hat{\mathcal{M}} B_0(0, M_Z^2, \hat{\mathcal{M}}^2) \mathbf{U}_L^\dagger, \quad (\text{A.7})$$

$$\delta\mathbf{M}_L^{(Z)}(2, 1) = -\frac{g^2}{64\pi^2 c_w^2 M_Z^2} \mathbf{U}_L^* \hat{\mathcal{M}}^3 B_0(0, \xi_Z M_Z^2, \hat{\mathcal{M}}^2) \mathbf{U}_L^\dagger, \quad (\text{A.8})$$

$$\delta\mathbf{M}_L^{(Z)}(2, 2) = \frac{g^2}{64\pi^2 c_w^2 M_Z^2} \mathbf{U}_L^* \hat{\mathcal{M}}^3 B_0(0, M_Z^2, \hat{\mathcal{M}}^2) \mathbf{U}_L^\dagger. \quad (\text{A.9})$$

As regards the G^0 and h^0 self-energies they are given by

$$\Sigma_L^{S(X)} = \mathbf{U}_L^T \delta\mathbf{M}_L^{(X)} \mathbf{U}_L \quad (X = G^0, h^0) \quad (\text{A.10})$$

with $\delta\mathbf{M}_L^{(X)}$ given by

$$\delta\mathbf{M}_L^{(G^0)} = \frac{g^2}{64\pi^2 c_w^2 M_Z^2} \mathbf{U}_L^* \hat{\mathcal{M}}^3 B_0(0, \xi_Z M_Z^2, \hat{\mathcal{M}}^2) \mathbf{U}_L^\dagger \quad (\text{A.11})$$

$$\delta\mathbf{M}_L^{(h^0)} = -\frac{g^2}{64\pi^2 c_w^2 M_Z^2} \mathbf{U}_L^* \hat{\mathcal{M}}^3 B_0(0, m_h^2, \hat{\mathcal{M}}^2) \mathbf{U}_L^\dagger. \quad (\text{A.12})$$

In the calculation of the above expressions we have used the relation

$$\mathbf{U}_R^\dagger \mathbf{M}_D = \hat{\mathcal{M}} \mathbf{U}_L^\dagger, \quad (\text{A.13})$$

that follows from the diagonalization relation (2.6) and the unitarity constraints of the matrix \mathbf{U} .

Some words are in order regarding these results. Corrections (A.8) and (A.11) cancel, ensuring the gauge invariance of the result. The Passarino-Veltman function B_0 has a finite and infinite part,⁵ the infinite piece in $\delta\mathbf{M}_L^{(Z)}(1)$ cancels due to the constraint

$$\mathbf{U}_L^* \hat{\mathcal{M}} \mathbf{U}_L = \mathbf{0}, \quad (\text{A.14})$$

whereas the divergent pieces in $\delta\mathbf{M}_L^{(Z)}(2,2)$ and $\delta\mathbf{M}_L^{(h^0)}$ cancel among them,⁶ thus demonstrating that $\delta\mathbf{M}_L$ is finite as anticipated in section 3. Taking into account that the finite part of B_0 can be recasted as

$$\begin{aligned} B_0^f(0, m_0^2, m_1^2) &= - \left[\frac{1}{m_1^2/m_0^2 - 1} \ln \left(\frac{m_1^2}{m_0^2} \right) + \ln m_1^2 \right] \\ &= - \left[\frac{m_1^2/m_0^2 \ln \left(\frac{m_1^2}{m_0^2} \right)}{m_1^2/m_0^2 - 1} + \ln m_0^2 \right] \end{aligned} \quad (\text{A.15})$$

the finite parts of $\delta\mathbf{M}_L^{(Z)}(1)$ and $\delta\mathbf{M}_L^{(Z)}(2,2)$ combine to yield

$$\delta\mathbf{M}_L^{(Z)f} = \frac{3g^2}{64\pi^2 M_W^2} \mathbf{U}_L^* \hat{\mathcal{M}}^3 \left(\frac{\hat{\mathcal{M}}^2}{M_Z^2} - \mathbf{1} \right)^{-1} \ln \left(\frac{\hat{\mathcal{M}}^2}{M_Z^2} \right) \mathbf{U}_L^\dagger. \quad (\text{A.16})$$

Finally the finite contribution from the Higgs self-energy function reads

$$\delta\mathbf{M}_L^{(h^0)f} = \frac{g^2}{64\pi^2 M_W^2} \mathbf{U}_L^* \hat{\mathcal{M}}^3 \left(\frac{\hat{\mathcal{M}}^2}{m_{h^0}^2} - \mathbf{1} \right)^{-1} \ln \left(\frac{\hat{\mathcal{M}}^2}{m_{h^0}^2} \right) \mathbf{U}_L^\dagger. \quad (\text{A.17})$$

The finite correction $\delta\mathbf{M}_L$, discussed in section 3, is obtained from the dominant parts of eqs. (A.16) and (A.17) (order $\hat{\mathbf{M}}_R^{-1}$). These pieces can be extracted by using eq. (A.13) and by taking into account that in the seesaw limit $\mathbf{M}_D \ll \mathbf{M}_R$, in the basis for which \mathbf{M}_R is diagonal, the matrix \mathbf{U}_R can be written as

$$\mathbf{U}_R = (-\xi^\dagger \mathbf{U}_\ell, \mathbf{1}), \quad (\text{A.18})$$

where $\xi = \mathbf{M}_D^T \mathbf{M}_R^{-1}$.

⁵Here by infinite part we mean $B_0^{(inf)}(0, m_0^2, m_1^2) = 2\epsilon^{-1} - \gamma + 4\pi + 1$.

⁶There is also a finite term, $\ln \hat{\mathcal{M}}^2$, that cancels.

References

- [1] T. Schwetz, M.A. Tortola and J.W.F. Valle, *Three-flavour neutrino oscillation update*, *New J. Phys.* **10** (2008) 113011 [[arXiv:0808.2016](#)] [[SPIRES](#)].
- [2] M.C. Gonzalez-Garcia, M. Maltoni and J. Salvado, *Updated global fit to three neutrino mixing: status of the hints of $\theta_{13} > 0$* , *JHEP* **04** (2010) 056 [[arXiv:1001.4524](#)] [[SPIRES](#)].
- [3] P. Minkowski, *$\mu \rightarrow e\gamma$ at a rate of one out of 1-billion muon decays?*, *Phys. Lett.* **B 67** (1977) 421 [[SPIRES](#)].
- [4] T. Yanagida, *Horizontal gauge symmetry and masses of neutrinos*, in the proceedings of the *Workshop on the Baryon Number of the Universe and Unified Theories*, Tsukuba Japan, 13–14 February 1979.
- [5] R.N. Mohapatra and G. Senjanović, *Neutrino mass and spontaneous parity nonconservation*, *Phys. Rev. Lett.* **44** (1980) 912 [[SPIRES](#)].
- [6] M. Gell-Mann, P. Ramond and R. Slansky, *Complex spinors and unified theories*, [CERN Print-80-0576](#).
- [7] J. Schechter and J.W.F. Valle, *Neutrino masses in $SU(2) \times U(1)$ theories*, *Phys. Rev.* **D 22** (1980) 2227 [[SPIRES](#)].
- [8] J.A. Casas and A. Ibarra, *Oscillating neutrinos and $\mu \rightarrow e, \gamma$* , *Nucl. Phys.* **B 618** (2001) 171 [[hep-ph/0103065](#)] [[SPIRES](#)].
- [9] S. Davidson and A. Ibarra, *Determining seesaw parameters from weak scale measurements?*, *JHEP* **09** (2001) 013 [[hep-ph/0104076](#)] [[SPIRES](#)].
- [10] W. Grimus and H. Neufeld, *Radiative neutrino masses in an $SU(2) \times U(1)$ model*, *Nucl. Phys.* **B 325** (1989) 18 [[SPIRES](#)].
- [11] A. Pilaftsis, *Radiatively induced neutrino masses and large Higgs neutrino couplings in the standard model with Majorana fields*, *Z. Phys.* **C 55** (1992) 275 [[hep-ph/9901206](#)] [[SPIRES](#)].
- [12] B.A. Kniehl and A. Pilaftsis, *Mixing renormalization in Majorana neutrino theories*, *Nucl. Phys.* **B 474** (1996) 286 [[hep-ph/9601390](#)] [[SPIRES](#)].
- [13] W. Grimus and H. Neufeld, *3-neutrino mass spectrum from combining seesaw and radiative neutrino mass mechanisms*, *Phys. Lett.* **B 486** (2000) 385 [[hep-ph/9911465](#)] [[SPIRES](#)].
- [14] W. Grimus and L. Lavoura, *Softly broken lepton numbers and maximal neutrino mixing*, *JHEP* **07** (2001) 045 [[hep-ph/0105212](#)] [[SPIRES](#)].
- [15] A. Pilaftsis, *Gauge and scheme dependence of mixing matrix renormalization*, *Phys. Rev.* **D 65** (2002) 115013 [[hep-ph/0203210](#)] [[SPIRES](#)].
- [16] W. Grimus and L. Lavoura, *Soft lepton-flavor violation in a multi-Higgs-doublet seesaw model*, *Phys. Rev.* **D 66** (2002) 014016 [[hep-ph/0204070](#)] [[SPIRES](#)].
- [17] W. Grimus and L. Lavoura, *One-loop corrections to the seesaw mechanism in the multi-Higgs-doublet standard model*, *Phys. Lett.* **B 546** (2002) 86 [[hep-ph/0207229](#)] [[SPIRES](#)].
- [18] J.A. Casas, J.M. Moreno, N. Rius, R. Ruiz de Austri and B. Zaldivar, *Fair scans of the seesaw. Consequences for predictions on LFV processes*, *JHEP* **03** (2011) 034 [[arXiv:1010.5751](#)] [[SPIRES](#)].

- [19] P.F. Harrison, D.H. Perkins and W.G. Scott, *Tri-bimaximal mixing and the neutrino oscillation data*, *Phys. Lett. B* **530** (2002) 167 [[hep-ph/0202074](#)] [[SPIRES](#)].
- [20] P. Huber and W. Winter, *Neutrino factories and the ‘magic’ baseline*, *Phys. Rev. D* **68** (2003) 037301 [[hep-ph/0301257](#)] [[SPIRES](#)].
- [21] A. Ibarra, E. Molinaro and S.T. Petcov, *TeV scale see-saw mechanisms of neutrino mass generation, the Majorana nature of the heavy singlet neutrinos and $\beta\beta$ -decay*, *JHEP* **09** (2010) 108 [[arXiv:1007.2378](#)] [[SPIRES](#)].
- [22] G. Passarino and M.J.G. Veltman, *One loop corrections for e^+e^- annihilation into $\mu^+\mu^-$ in the Weinberg model*, *Nucl. Phys. B* **160** (1979) 151 [[SPIRES](#)].